NANO LETTERS

2005
Vol. 5, No. 6
1175−1179

Combined Optical Tweezers/Ion Beam Technique to Tune Colloidal Masks for Nanolithography

Dirk L. J. Vossen,*,†,‡ Damir Fific,† Joan Penninkhof,† Teun van Dillen,† Albert Polman,*,† and Alfons van Blaaderen*,‡

Center for Nanophotonics, FOM Institute AMOLF, Kruislaan 407, 1098 SJ Amsterdam, The Netherlands, and Soft Condensed Matter, Debye Institute, Utrecht University, Princetonplein 5, 3584 CC Utrecht, The Netherlands

Received March 4, 2005; Revised Manuscript Received April 11, 2005

ABSTRACT

A method is presented to control the in-plane ordering, size, and interparticle distance of nanoparticles fabricated by evaporation through a mask of colloidal particles. The use of optical tweezers combined with critical point drying gives single-particle position control over the colloidal particles in the mask. This extends the geometry of the colloidal masks from (self-organized) hexagonal to any desired symmetry and spacing. Control over the mask's hole size is achieved by MeV ion irradiation, which causes the colloids to expand in the in-plane direction, thus shrinking the size of the holes. After modification of the mask, evaporation at different angles with respect to the mask gives additional control over structure and interparticle distance, allowing nanoparticles of different materials to be deposited next to each other. We demonstrate large arrays of metal nanoparticles with dimensions in the 15–30 nm range, with control over the interparticle distance and in-plane ordering.

Arrays of nanoparticles can find applications in photonic, electronic, magnetic, and sensor devices.[1−6] Conventional methods used to fabricate structures of nanoparticles (such as electron beam lithography) are complex, expensive, time-consuming. An alternative method to create arrays of small particles on a substrate is nanosphere lithography (NSL). This technique was pioneered in the early 1980s[7,8] and was further developed by several groups.[9,10] In NSL, a self-organized layer of colloidal spheres is used as a mask for a lithographic step such as illumination, deposition, or etching. When used as a deposition mask, an array of particles is left on the substrate after removal of the colloidal mask. NSL is a simple, fast, and inexpensive method to create large arrays of particles on a substrate. Typical feature sizes after removal of the mask are 100 nm and above. Arrays of metallic nanoparticles created with NSL were used to study plasmonic resonances[11] and to fabricate plasmonic sensors.[12] Surfaces patterned with colloidal masks have also been used for catalyzing the growth of nanofibers (e.g., of carbon[13] and ZnO[14]) and for selective protein adsorption.[15] More complex structures of particles can be created using multiple depositions at different angles[16] or by rotating the sample during deposition.[17]

Nanosphere lithography has two major disadvantages.[9,10] First, the geometry of the mask of colloidal particles is limited since it is created by self-organization: for a single layer the only structure is hexagonal close packed. Second, the size and spacing of the mask holes are coupled, and thus these properties cannot be independently controlled.

In this paper we present a combination of two methods to resolve these limitations of nanosphere lithography: we create colloidal masks with arbitrary geometry using optical tweezers, and tune the shape of the mask using ion irradiation. In this way, the in-plane ordering as well as the size and interparticle distance of nanoparticles formed by evaporation through the mask can be controlled.

To create masks with arbitrary geometry, glass or silicon substrates were given a positive surface charge and then patterned with negatively charged colloidal silica particles using optical tweezers.[18,19] Glass microscope cover slides (diameter 19 mm, Chance, thickness #1) and Si(100) wafers were used as received. These substrates were immersed in a mixture of 170 mL ethanol and 4.5 mL ammonia (29 wt. %). Then 23.5 mL 3-aminopropyl triethoxysilane was added and the substrate was let to react for 1.5 h under stirring. All chemicals were analytical grade, obtained from Merck, and used as received. The substrate was then taken from the mixture and rinsed with ethanol. A sample cell was prepared by sandwiching a drop of colloidal dispersion between a (uncoated) glass microscope cover slide and a coated

* Corresponding authors. E-mail: d.l.j.vossen@phys.uu.nl; polman@amolf.nl; a.vanblaaderen@phys.uu.nl; www.colloid.nl and www.erbium.nl.
† FOM Institute AMOLF.
‡ Utrecht University.

10.1021/nl050421k CCC: $30.25
Published on Web 05/10/2005

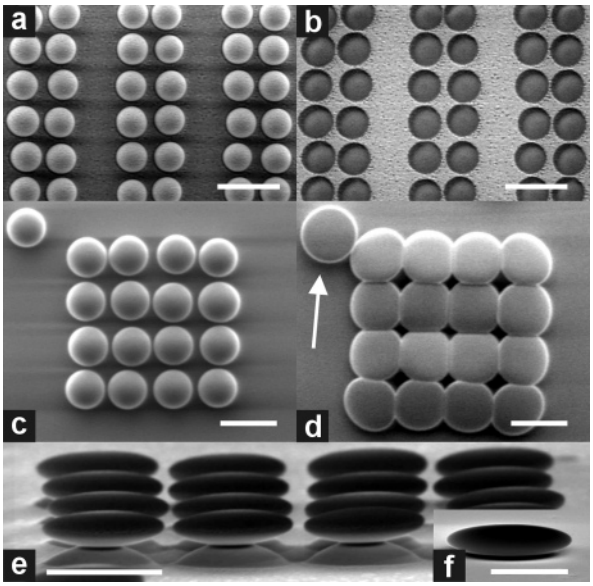

Figure 1. Colloidal masks made with single-particle position control using optical tweezers, and then modified with 4 MeV Xe ion irradiation. (a) SEM image of 1.0 μm diameter silica particles positioned on a glass substrate using optical tweezers. The sample was dried using critical point drying and covered with a 10 nm thick silver layer by thermal evaporation. (b) After removal of the particles with sonication, the structure of the mask was replicated on the substrate. (c) 1.4 μm diameter silica particles positioned with square symmetry. (d) Same structure after normal-incidence irradiation with 4 MeV Xe ions to a fluence of 2.0×10^{15} cm^{-2} at 90 K. The in-plane expansion of the colloidal particles can be tuned by varying the ion fluence. (e) Side-view of an array of ion beam deformed 1.4 μm diameter silica colloids (4 MeV, 2.0×10^{15} cm^{-2}) imaged at an angle of 10° with respect to the substrate. Not only the silica particles but also the glass substrate was deformed. The size aspect ratio of the particles was 3.4. (f) Side-view (at 10°) of a ion beam deformed 1.4 μm diameter silica colloids (4 MeV) on a silicon substrate. Note that the silicon substrate did not deform, while the silica particle deformed as in Figure 1e. Scale bars in Figure 1a−1e are 2 μm; scale bar in Figure 1f is 1 μm.

substrate. Silica particles with a diameter of 1.0 μm or 1.4 μm and a polydispersity less than a few percent were synthesized using a Stöber growth process and subsequent growth steps using methods described in detail elsewhere.[20−22] The size and polydispersity were determined using scanning electron microscopy (SEM, FEI XL30 SFEG, 1−15 keV) on several hundreds of particles. Optical tweezers were used to position negatively charged colloidal particles, taken from a reservoir at the bottom of the sample, on the positively charged substrate.[18] The optical tweezers setup is described in detail elsewhere.[23]

This optical tweezers method allows masks to be created with control over the position of single particles. After patterning, the sample is removed from the solvent using critical point drying (CPD, Bal-tec; CPD 030) to prevent capillary forces from breaking up the structure.[19] Figure 1a shows an SEM image of a double-line array of 1.0 μm diameter silica particles on a glass substrate after patterning and drying. The average center-to-center distance between nearest neighbors within each line was 1.2 μm. A 10 nm thick silver layer was deposited onto the colloidal mask by thermal evaporation at a base pressure of 1.3×10^{-6} mbar. The same section of the substrate is shown in Figure 1b after the mask was removed by sonication in ethanol. Clearly, the mask was replicated in the silver layer on the substrate. The method can be used to create more complex masks in which colloidal particles of different size, shape, and composition can be incorporated.[23,24]

Additional control over the mask's dimensions can be achieved by ion irradiation. As we have shown earlier, under irradiation with an MeV ion beam individual colloidal particles expand in the plane perpendicular to the ion beam and shrink parallel to the ion beam.[25] This plastic deformation effect can be used to tune the size and shape of the holes in the colloidal deposition mask. Figure 1c shows an SEM image of a cubic mask pattern created with optical tweezers and CPD on a glass substrate. The center-to-center distance between the 1.4 μm diameter silica particles was 1.6 μm. The same structure is shown at the same magnification in Figure 1d after irradiation, perpendicular to the substrate, with 4 MeV Xe^+ ions to a fluence of 2.0×10^{15} cm^{-2} using a 1 MV van de Graaff accelerator. During irradiation the sample was clamped on a copper substrate that was cooled to 90 K using liquid nitrogen. The base pressure during irradiation was 5×10^{-7} mbar.

Clearly, the ion beam induced deformation has dramatically shrunk the size of the holes between the colloids. The radial axis of the projection of the particle just outside the structure (marked with an arrow) increased from 1.4 μm to 2.0 μm. When the deforming spheres in a mask come into contact, the deformation becomes a collective process and the final dimensions are determined by the combined deformation of interacting colloids. This can be clearly seen in Figure 1d where the shapes of the colloidal particles and the holes depend on their position in the mask. In Figure 1d, the center-to-center distance in the mask pattern is 1.8 μm, much larger than the original spacing of 1.6 μm (Figure 1c). This indicates that during irradiation the expansion of the interacting colloids caused an overall expansion of the mask domain, with colloids sliding over the substrate. For large domains, buckling of the colloidal mask was observed in some cases, which we attribute to large in-plane stresses resulting from the deformation.[27]

A more open structure of silica particles is shown in Figure 1e at a viewing angle of 10° with the substrate. The colloidal mask was irradiated with 2.0×10^{15} 4 MeV Xe ions/cm^2. The average penetration depth of these ions in colloidal silica was calculated to be 1.7 μm, using TRIM98, a Monte Carlo simulation program.[26]

The size aspect ratio (major over minor axis) of the colloidal particles in the mask increased from 1 to 3.4. From Figure 1e it can also be seen that the glass substrate deformed under irradiation, leading to the formation of a pedestal centered under each colloid. We attribute this to inhomogeneous anisotropic deformation of the substrate under the mask. For 4 MeV Xe, the energy remaining after penetration through the center of a colloid is only 0.85 MeV. As the deformation rate increases with ion energy,[28] the driving force for in-plane expansion of the substrate surface layer under the colloids will be much smaller than under the holes (where

the ion energy is 4 MeV). This can lead to a plastic shape deformation of the glass substrate that causes formation of pedestals under each colloid.

To verify this hypothesis, a glass substrate covered with 1.0 μm diameter colloidal particles was irradiated with 30 MeV Cu^{5+} ions (8.7×10^{14} cm^{-2}) using a 6 MV tandem accelerator. The average penetration depth of these ions was calculated to be 8.6 μm.[26] At this high energy, the relative energy loss through the colloids is small, so that the substrate is irradiated at a nearly uniform energy. Indeed, under these conditions the substrate was found to stay flat.

The substrate deformation observed for 4 MeV Xe irradiation can be avoided by using silicon as a substrate. Crystalline Si rapidly becomes amorphous under 4 MeV Xe irradiation, and as we have recently shown,[29] the anisotropic deformation rate of amorphous silicon is ~10 times smaller than that of silica. Indeed, (amorphized) silicon substrates covered with 1.4 μm diameter silica colloids stayed flat for an ion fluence of 2.0×10^{15} Xe cm^{-2}. Figure 1f shows a silica particle on a silicon substrate after irradiation with intermediate ion fluence. It can clearly be seen that the silicon substrate remained flat, while the deformation of silica particle is comparable to that of the particles in Figure 1e. While the formation of pedestals may be considered as unwanted (and can be avoided as we have shown above), we note that ellipsoidal colloidal particles on a pedestal may find use as arrays of (coupled) optical microresonators.[30]

Figure 2a shows an SEM image of a two-dimensional hexagonal mask of 1.4 μm diameter silica particles on a silicon substrate. The mask was irradiated with 6×10^{14} MeV Xe ions/cm^2. Due to this irradiation, the size of the holes decreased from 400 nm (unirradiated) to 190 nm. Hole sizes were determined at least five or six rows of particles away from the domain edges and an average over five holes was taken. We define the size of a hole between three colloidal particles in a hexagonal close-packed mask as the smallest distance between the point where two particles touch and a point on the surface of the third colloidal particle (see the inset in the lower left corner of Figure 2a). The dependence of the size of holes in a colloidal mask on the ion fluence was determined for a two-dimensional hexagonal lattice of close-packed 1.4 μm diameter silica particles on a silicon substrate. The mask, with crystalline domains with dimensions between 20 and 50 μm, was formed by self-organization during slow evaporation of a drop of a colloidal dispersion on a silicon substrate. During 4 MeV Xe ion irradiation the sample was gradually moved along the 2.5 × 2.5 cm^2 aperture through which the ion beam was scanned. A linearly varying ion fluence ranging from zero to 1.2×10^{15} ions/cm^2 across the sample area was thus created. As can be seen in Figure 2b, the hole size decreases with ion fluence, as a result of the increased in-plane particle expansion. The insets in the top of Figure 2b show an unirradiated section of the mask, and sections irradiated with 3.3×10^{14}, 6.5×10^{14}, and 13×10^{14} ions/cm^2. The corresponding hole sizes are 400, 330, 137, and 0 nm, respectively. Small variations in hole size observed at each fluence are attributed to polydispersity in colloid size.

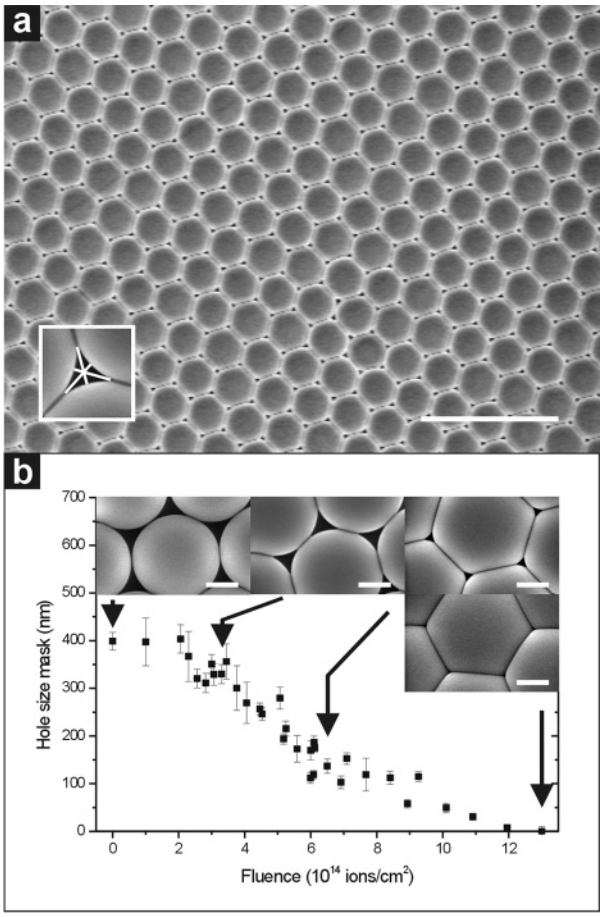

Figure 2. Colloidal masks of 1.4 μm diameter silica particles on a silicon substrate modified with 4 MeV Xe ion irradiation. (a) SEM image of a mask irradiated with 6×10^{14} ions/cm^2. The size of the holes was 190 nm. The inset in the lower left corner shows how the hole size is defined. (b) Dependence of hole size in a two-dimensional hexagonal mask irradiated with 4 MeV Xe ions. The size of the holes gradually decreased until the holes were completely closed. The insets at the top of the image show SEM images of the mask at fluences of 0, 3.3×10^{14}, 6.5×10^{14}, and 12×10^{14} ions/cm^2; corresponding hole sizes were 400, 330, 137, and 0 nm, respectively. The arrows indicate the fluences at which the images were taken. Scale bar in Figure 2a is 5 μm; all other scale bars are 500 nm.

To demonstrate that the ion beam deformed colloidal mask can be used to fabricate nanostructures, a 30 nm thick gold layer was deposited by electron beam evaporation (base pressure 1×10^{-8} mbar) onto various ion irradiation-modified hexagonal masks (colloid diameter 1.4 μm, 4 MeV Xe). Subsequently, the colloidal mask was removed by sonication. As a reference, Figure 3a shows a deposited pattern for an unirradiated mask. The size of these gold particles was 400 nm. Figures 3b, 3c, and 3d show arrays of gold particles made using masks irradiated at 4.9×10^{14}, 7.7×10^{14}, and 11×10^{14} ions/cm^2, respectively, leading to gold particle sizes of 229, 119, and 30 nm. The variation in nanoparticle size is 5−10%. A high-magnification image shows a Au dot with feature sizes between 15 and 20 nm (Figure 3e). As can be seen, for these small particles, inhomogeneous particle shapes are observed, which are attributed to the nucleation and growth kinetics. Thermal annealing can remove sharp features and combine metal

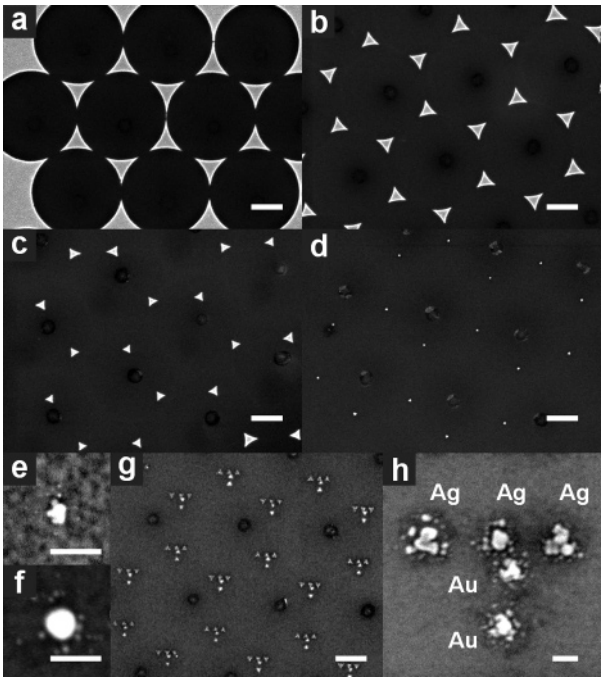

Figure 3. Arrays of metal nanoparticles created with an ion beam deformed mask. (a) Hexagonal array of gold particles with a size of 400 nm, created on a glass substrate using an unmodified colloidal mask of 1.4 μm diameter silica particles. (b) Hexagonal array of gold particles with a size of 229 nm, (c) 119 nm, and (d) 30 nm created with a mask modified with 4 MeV Xe ions. (e) Image at high magnification of a Au particle with feature sizes of 15−20 nm. (f) Image of a Au particle annealed at 150 °C and 250 °C (both for 30 min). The particle has a more round and single droplet like shape. (g) Array of "T" structures with three silver and two gold nanoparticles created by deposition at different angles on a modified mask. (h) Image at high magnification of a "T" structure. The size of the particles is between 50 and 80 nm and their spacing is ∼135 nm. Scale bars in Figure 3a−d and 3g are 500 nm; in Figure 3e−f, and 3h are 50 nm.

nanoparticles that are close together.[31] Figure 3f shows a Au particle that was annealed in air at ambient pressure at 150 °C for 30 min and subsequently at 250 °C for another 30 min. The particle shows a more round shape and has become a single droplet-shaped particle.

To further demonstrate the versatility of the combination of optical tweezers and ion irradiation, more complex nanoparticle arrays were created by subsequent deposition of metals at different angles using an ion beam modified mask. Figure 3g shows an array of "T" structures made through subsequent silver and gold depositions through an ion-modified mask, where different depositions were done at two sets of orthogonal angles. Three silver particles were created by deposition of 11 nm silver at angles of −4.5, 0, and +4.5 degrees in a horizontal plane in Figure 3g. Two gold particles were made using a subsequent deposition of 10.5 nm gold at angles of −4.5 and 0 degrees in a vertical plane in Figure 3g. Figure 3h shows a single "T" structure at higher magnification. The size of the core of the deposited features was in the range 30−50 nm and the center-to-center interparticle spacing was ∼135 nm. The spacing between the closest silver and gold nanoparticles was 62 nm. Annealing of the structure in Figure 3g and 3h, composed of both silver and gold dots, was not possible due to the different annealing kinetics of the two metals. However, metal dots in more complex structures such as "T" structures composed of a single metal are expected to change shape after annealing as shown in Figure 3f and reference 31. Finally, we note that during deposition the mask hole size is gradually decreasing, due to the continued deposition of metal on the colloids in the mask. Thus for very small holes, the total amount of metal that is deposited for each particle is determined by a self-limiting process.

In conclusion, we have provided a solution to two major limitations of nanosphere lithography. The geometry of the masks is extended from (self-organized) hexagonal close-packed to any desired symmetry using optical tweezers combined with critical point drying. In the present experiments colloidal particles were positioned in the mask by manual control, but the process can be fully automated to achieve a higher accuracy as well an increased speed of patterning. Control over the hole size (independent of the size of the colloids in the mask) is achieved by ion irradiation, which causes an in-plane expansion of the mask, thus shrinking the size of the holes. By varying the ion fluence, the hole size can be continuously reduced to arbitrarily small size. In this way, hole size and spacing can be arbitrarily controlled. Recently, we have shown that deformation of colloidal spheres is also effective at ion energies below 300 keV.[28] Accelerators with such ion energies are readily available. The modified masks can be used to create arrays of nanoparticles with sizes down to tens of nanometers. Evaporation of material at different angles with respect to the mask gives additional control over structure and interparticle distance, allowing nanoparticles of different materials to be arranged with high accuracy in a variety of geometries.

Acknowledgment. We gratefully acknowledge the assistance of Jan Verhoeven with metal evaporations. We thank Michiel de Dood, Jacob Hoogenboom, and Anna Tchebotareva for discussions. Jan Verhoeven, Daniël Vanmaekelbergh, and Arnout Imhof are thanked for critical reading of the manuscript. This work is part of the research program of the "Stichting voor Fundamenteel Onderzoek der Materie (FOM)", which is financially supported by the "Nederlandse organisatie voor Wetenschappelijk Onderzoek (NWO)".

References

(1) Shipway, A. N.; Katz, E.; Willner, I. *ChemPhysChem* **2000**, *1*, 18.
(2) Rogach, A. L.; Talapin, D. V.; Shevchenko, E. V.; Kornowski, A.; Haase, M.; Weller, H. *Adv. Funct. Mater.* **2002**, *12*, 653.
(3) Redl, F. X.; Cho, K. S.; Murray, C. B.; O'Brien, S. *Nature* **2003**, *423*, 968.
(4) Schaller, R. D.; Petruska, M. A.; Klimov, V. I. *J. Phys. Chem. B* **2003**, *107*, 13765.
(5) Alivisatos, A. P. *Nat. Biotechnol.* **2004**, *22*, 47.
(6) Maier, S. A.; Kik, P. G.; Atwater, H. A.; Meltzer, S.; Harel, E.; Koel, B. E.; Requicha, A. A. G. *Nat. Mater.* **2003**, *2*, 229.
(7) Fischer, U. C.; Zingsheim, H. P. *J. Vac. Sci. Technol.* **1981**, *19*, 881.
(8) Deckman, H. W.; Dunsmuir, J. H. *Appl. Phys. Lett.* **1982**, *41*, 377.
(9) Hulteen, J. C.; Van Duyne, R. P. *J. Vac. Sci. Technol. A* **1995**, *13*, 1553.
(10) Burmeister, F.; Schafle, C.; Matthes, T.; Bohmisch, M.; Boneberg, J.; Leiderer, P. *Langmuir* **1997**, *13*, 2983.

(11) Haynes, C. L.; Van Duyne, R. P. *J. Phys. Chem. B* **2001**, *105*, 5599.
(12) Malinsky, M. D.; Kelly, K. L.; Schatz, G. C.; Van Duyne, R. P. *J. Am. Chem. Soc.* **2001**, *123*, 1471.
(13) Huang, Z. P.; Carnahan, D. L.; Rybczynski, J.; Giersig, M.; Sennett, M.; Wang, D. Z.; Wen, J. G.; Kempa, K.; Ren, Z. F. *Appl. Phys. Lett.* **2003**, *82*, 460.
(14) Wang, X.; Summers, C. J.; Wang, Z. L. *Nano Lett.* **2004**, *4*, 423.
(15) Michel, R.; Reviakine, I.; Sutherland, D.; Fokas, C.; Csucs, G.; Danuser, G.; Spencer, N. D.; Textor, M. *Langmuir* **2002**, *18*, 8580.
(16) Haynes, C. L.; McFarland, A. D.; Smith, M. T.; Hulteen, J. C.; Van Duyne, R. P. *J. Phys. Chem. B* **2002**, *106*, 1898.
(17) Kosiorek, A.; Kandulski, W.; Chudzinski, P.; Kempa, K.; Giersig, M. *Nano Lett.* **2004**, *4*, 1359.
(18) Hoogenboom, J. P.; Vossen, D. L. J.; Faivre-Moskalenko, C.; Dogterom, M.; van Blaaderen, A. *Appl. Phys. Lett.* **2002**, *80*, 4828.
(19) Vossen, D. L. J.; Hoogenboom, J. P.; Overgaag, K.; van Blaaderen, A. In *Materials Research Society Symposium Proceedings*; Merhari, L., Ed.; Boston, 2002.
(20) van Blaaderen, A.; Vrij, A. *Langmuir* **1992**, *8*, 2921.
(21) van Blaaderen, A.; van Geest, J.; Vrij, A. *J. Colloid Interface Sci.* **1992**, *154*, 481.
(22) Giesche, H. *J. Eur. Ceram. Soc.* **1994**, *14*, 205.
(23) Vossen, D. L. J.; van der Horst, A.; Dogterom, M.; van Blaaderen, A. *Rev. Sci. Instrum.* **2004**, *75*, 2960.
(24) van Blaaderen, A.; Hoogenboom, J. P.; Vossen, D. L. J.; Yethiraj, A.; van der Horst, A.; Visscher, K.; Dogterom, M. *Faraday Discuss.* **2003**, *123*, 107.
(25) Snoeks, E.; van Blaaderen, A.; van Dillen, T.; van Kats, C. M.; Brongersma, M. L.; Polman, A. *Adv. Mater.* **2000**, *12*, 1511.
(26) Ziegler, J. F.; Biersack, J. P.; Littmark, U. *The stopping and range of ions in solids*; Pergamon: New York, 1985.
(27) Snoeks, E.; Weber, T.; Cacciato, A.; Polman, A. *J. Appl. Phys.* **1995**, *78*, 4723.
(28) van Dillen, T.; Polman, A.; van Kats, C. M.; van Blaaderen, A. *Appl. Phys. Lett.* **2003**, *83*, 4315.
(29) van Dillen, T.; de Dood, M. J. A.; Penninkhof, J. J.; Polman, A.; Roorda, S.; Vredenberg, A. M. *Appl. Phys. Lett.* **2004**, *84*, 3591.
(30) Vahala, K. J. *Nature* **2003**, *424*, 839.
(31) Burmeister, F.; Badowsky, W.; Braun, T.; Wieprich, S.; Boneberg, J.; Leiderer, P. *Appl. Surf. Sci.* **1999**, *145*, 461.

NL050421K